Available online at www.sciencedirect.com
SCIENCE DIRECT®
PERGAMON
Journal of Asian Earth Sciences 22 (2003) 363–381
Journal of Asian Earth Sciences
www.elsevier.com/locate/jseaes

Age, petrogenesis and significance of 1 Ga granitoids and related rocks from the Sendra area, Aravalli Craton, NW India

M.K. Pandit[a], L.M. Carter[b], L.D. Ashwal[c,*], R.D. Tucker[d], T.H. Torsvik[e], B. Jamtveit[f], S.K. Bhushan[g]

[a]*Department of Geology, University of Rajasthan, Jaipur 302 004, India*
[b]*Lakefield Research Africa, P.O. Box 82582, Southdale, South Africa*
[c]*School of Geosciences, University of the Witwatersrand, Private Bag 3, Johannesburg WITS 2050 South Africa*
[d]*Department of Earth and Planetary Sciences, Washington University, St. Louis, MO 63130, USA*
[e]*VISTA, c/o Geological Survey of Norway, Leif Erikssons vei 39, N-7491 Trondheim, Norway*
[f]*Department of Geology, University of Oslo, P.O. Box 1047, Blindern N-0316, Norway*
[g]*Geological Survey of India, International Wing, Jawaharlal Nehru Road, Kolkata 700 016, India*

Received 1 July 2002; revised 31 January 2003; accepted 3 February 2003

Abstract

We present new geochronological, petrological, geochemical and isotopic data for granitic and related rocks from the Aravalli Craton, Rajasthan, northwestern India. In the Sendra area, five variably deformed granitoid plutons, ranging in composition from tonalite to granite, cut across carbonate-rich metasedimentary rocks of the Delhi Supergroup. The largest of these bodies, the Chang pluton (~15 km^2) is dominated by monzogranitic gneisses and aplitic dykes, composed of subequal proportions of quartz, plagioclase (An_{7-20}) and microcline (Or_{92-98}), with lesser biotite ($Fe^* = 0.8–0.9$) and accessory muscovite ($Fe^* = 0.7–0.8$). U–Pb zircon data (TIMS method) for a biotite granite gneiss yield a weighted mean $^{207}Pb/^{206}Pb$ age of 967.8 ± 1.2 Ma, which we interpret as representing the time of magmatic crystallization. Rb–Sr whole-rock isotopic data for the Chang pluton, including new analyses as well as previously published ones, yield a regression of 906 ± 67 Ma (MSWD = 82), which is barely within error of the U–Pb age. There is evidence for open-system behaviour in the Rb–Sr system, particularly for whole-rock samples with low Sr concentrations, and consequently high Rb/Sr. Sm–Nd isotopic data fail to yield meaningful age information. Initial isotopic ratios (at 968 Ma) for Chang pluton granitoids ($I_{Sr} = 0.7110 \pm 14$; $\varepsilon_{Nd} = -3.28 \pm 0.47$) are compatible with source materials similar to Archaean amphibolitic rocks of the Banded Gneiss Complex. Spatially associated with the Chang pluton is a massive metagabbro, composed of plagioclase (An_{45-68}) and magnesio-hornblende ($Fe^* = 0.3–0.4$), with secondary Cl-rich scapolite and ferrian zoisite. The scapolite and zoisite likely crystallized from metamorphic fluids that interacted with nearby calc-silicate schists and gneisses of the Delhi Supergroup. Aside from slight enrichments in Rb, U, Th and Ba, this metagabbro retains a primitive chemical signature similar to N-MORB (LREE depletion, low K), and initial isotopic ratios ($I_{Sr} = 0.7058$; $\varepsilon_{Nd} = +2.9$) that approach model depleted mantle at 968 Ma. The metagabbro is chemically and isotopically similar to mafic metavolcanic and related rocks that have been considered to represent ocean-floor and island-arc basaltic magmas. All available data are compatible with the idea that these rocks represent the products of convergent margin processes during the Early Neoproterozoic, a conclusion that could have important implications for the construction of the Rodinia supercontinent.

Keywords: Aravalli Craton; Rajasthan; Granitic rocks; Geochronology; Geochemistry; Isotope systematics

1. Introduction and geological overview

Understanding the origin and evolution of Precambrian terranes generally starts with geological mapping efforts that lead to the establishment of basement–cover relationships, and the recognition and characterization of intrusive and metamorphic events. In many cases, a diverse set of sedimentary, igneous and metamorphic events must be sorted out, the complexity of which varies substantially. One goal of such efforts is to establish reasonable controls on operative tectonic processes, and their temporal evolution. Although careful fieldwork can distinguish the *relative* timing of events, their *absolute* ages require

* Corresponding author. Tel.: +27-11-717-6652; fax: +27-22-717-6579.
E-mail address: ashwall@geosciences.wits.ac.za (L.D. Ashwal).

1367-9120/03/$ - see front matter © 2003 Elsevier Ltd. All rights reserved.
doi:10.1016/S1367-9120(03)00070-1

geochronology. With the precision that is now obtainable, particularly with U–Pb isotopic methods, geochronology can be used productively to constrain the timing as well as the rates of geological and tectonic processes, and in some cases to resolve contentious geological or stratigraphic relationships. Applications of these methods, in concert with geological, petrological, geochemical and geophysical studies, have resulted in great advances in the understanding of some Precambrian terranes, such as the Canadian Shield. Many other terranes, however, particularly those in countries of the southern tier, still await such studies. In this paper, we contribute to this for the Aravalli Craton of northwestern India, by reporting new U–Pb data, complemented with geochemical, isotopic and petrologic data, for granitoid and related rocks of Rajasthan.

The pioneering geological characterization of the Aravalli Craton, exposed over 80,000 km^2 in the states of Rajasthan and northern Gujarat (Fig. 1), was carried out by geologists of the Geological Survey of India (e.g. Coulson, 1933; Gupta, 1934; Gupta and Mukherjee, 1938; Heron, 1953). A recent summary can be found in Gupta et al. (1997), with useful geological maps at a scale of 1:250,000 (Gupta et al., 1995). Basement rocks, referred to as the Banded Gneiss Complex (BGC), consist dominantly of amphibolite to granulite grade, tonalitic to granodioritic gneisses, with associated lenticular masses of amphibolite (Heron, 1953). These rocks have yielded Sm–Nd ages between 3.3 ± 0.07 and 2.83 ± 0.05 Ga (Gopalan et al., 1990; Tobisch et al., 1994). Results from zircon dating for a variety of granitoids and gneisses yield results between 3281 ± 3 and 2440 ± 7 Ma (^{207}Pb/^{206}Pb ion microprobe methods, Wiedenbeck and Goswami, 1994; Wiedenbeck et al., 1996), and 3230–2620 Ma (zircon evaporation methods, Roy and Kröner, 1996). Two supracrustal sequences, both of which include metasedimentary and metavolcanic rocks, post-date the BGC; these are the Aravalli Supergroup, of presumed Palaeoproterozoic (2.5–1.7 Ga) age, and the Delhi Supergroup, of presumed Meso-to Neoproterozoic (1.7–0.6 Ga) age. Contact relationships within and between these supracrustal rocks are equivocal, as are their structural relationships to the BGC (e.g. Ahmad and Tarney, 1994). The Aravalli Supergroup was considered by Heron (1953) and Roy et al. (1988) to unconformably overlie the BGC, although Naha and Halyburton (1974) and Naha and Roy (1983) interpreted the boundary as a migmatization front. Similarly, the contact between the Aravalli and Delhi Supergroups has been discussed as an unconformity (Heron, 1953), or as a suture representing the closure of a Proterozoic ocean (Sugden et al., 1990).

Supracrustal rocks of the Delhi Supergroup are cut across by numerous, variably deformed granitoid plutons, ranging in size from <2 to >300 km^2, which were collectively referred to by Heron (1953) as the 'Erinpura granites'. Subsequently, on the basis of (regrettably unpublished) Rb–Sr whole-rock data (Choudhary et al., 1984), these granitoids were divided into an older group (~1.5–1.7 Ga) that evidently is spatially restricted to the northeastern exposures of the Delhi Supergroup, and a younger group (~0.75–0.85 Ga), which occurs southwest of Ajmer (Fig. 1). In current usage, the Erinpura granites refer specifically to the volumetrically more abundant younger group (Sinha Roy et al., 1998). The spatial and temporal separation of granitoids has led to the suggestion that sedimentation within the Delhi Supergroup was widely separated in space and time, with the northeastern part of the belt representing a Mesoproterozoic basin, and the southwestern exposures representing a Neoproterozoic one (Bose, 1989). This possibility is difficult to evaluate, given the general paucity of well-constrained and well-documented geochronological data. We report here the first precise U–Pb zircon age data for granitoids of the younger (Erinpura) group, and discuss their petrogenesis and significance, based on new chemical, petrologic and isotopic data. Details of the geology and relevant previous results for the Delhi Supergroup and crosscutting granitoids are presented in Section 2.

The youngest of the Precambrian magmatic sequences in the Aravalli Craton is referred to as the Malani Igneous Suite, which represents the world's third largest felsic volcanic/plutonic province (Pareek, 1981; Bhushan, 2000). These rocks, exposed over ~51,000 km^2, consist dominantly of undeformed and unmetamorphosed rhyolitic and rhyodacitic volcanics, and associated granitoid intrusives, which clearly unconformably overlie or intrude into metasediments of the Delhi Supergroup. Rb–Sr whole-rock isochrons of 730 ± 10 Ma were obtained by Crawford and Compston (1970). Our research group has initiated a petrological, geochronological and palaeomagnetic study of the Malani Igneous Suite, and some of our new results have already been published (e.g. Torsvik et al., 2001).

2. Local geological setting and previous work

Rocks of the Delhi Supergroup, which are variably exposed in the Aravalli Mountains as a NE–SW trending linear belt >700 km long between Delhi and Mt. Abu, southwest of Udaipur (Fig. 1), consist mainly of clastic and chemical metasediments (Gupta et al., 1997) that have been tightly folded into a regional synclinorium (Heron, 1953). There is evidence for polyphase deformation, and metamorphic grade varies from greenschist to upper amphibolite. There have been several attempts at stratigraphic subdivision and correlation that vary in detail (e.g. Heron, 1917, 1953; Gupta et al., 1997); we follow the stratigraphic classification and nomenclature of Gupta et al. (1997). The lowermost units (Gogunda Group) are dominated by clastic metasediments, including quartzites, arkosic schists and metaconglomerates. These rocks are overlain by carbonate-bearing units (Kumbhalgarh Group), dominantly

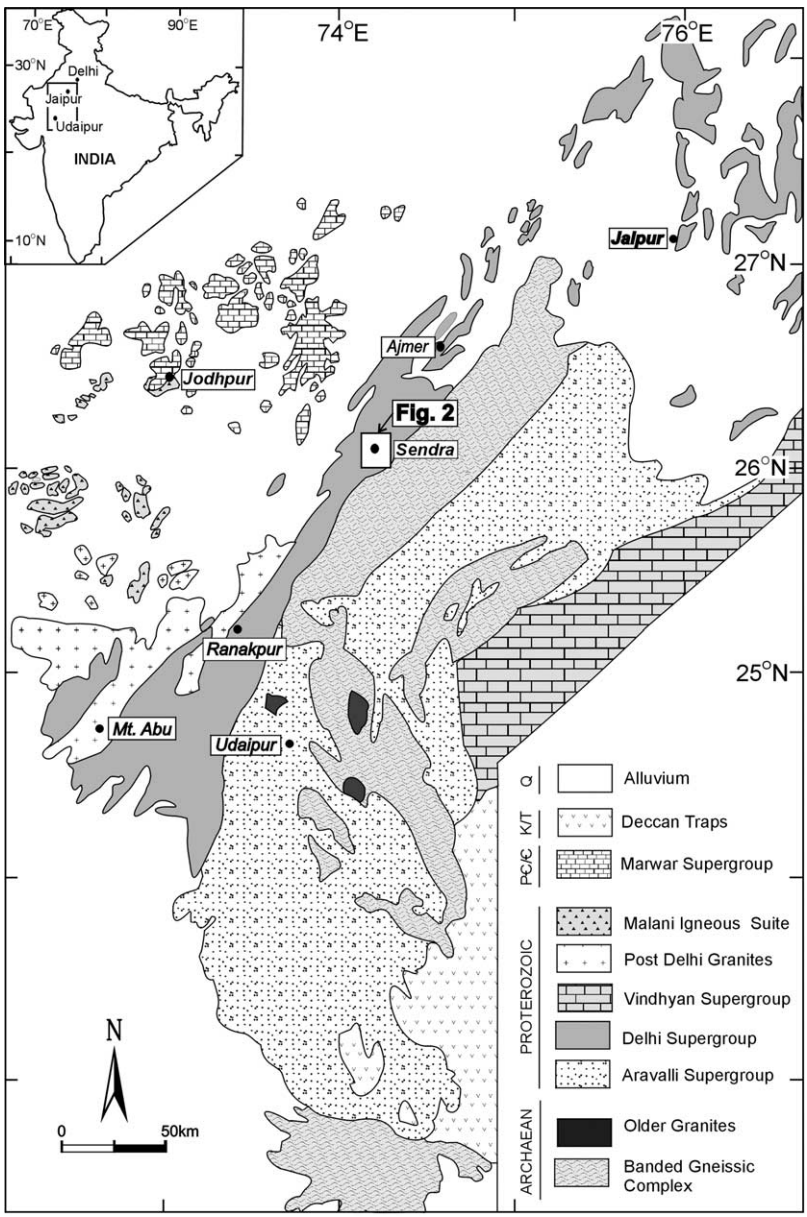

Fig. 1. Regional map of the Aravalli Craton, adapted from Heron (1953), Sharma (1995), and Roy and Kataria (1999), and maps published by the Geological Survey of India. Location of study area (Fig. 2) is indicated.

calc-silicate schists and gneisses, and biotite schists, with lesser marbles and quartzites. Infolded with the calc-silicate gneisses of the Kumbhalgarh Group are a series of amphibolitic mafic to ultramafic rocks; these have been interpreted as metabasalts and metagabbros, and have been discussed in terms of a possible ophiolitic origin based on their geochemical affinities to MORB and island-arc basalts (Phulad Ophiolite Series, Volpe and Macdougall, 1990). The uppermost units of the Delhi Supergroup include phyllites and schists of the Sirohi Group, which are overlain by the Punagarh and Sindreth Groups, characterized by siliciclastic sediments with associated basaltic to rhyolitic volcanic rocks. Given the paucity of well-constrained age information, it is difficult to evaluate these stratigraphic relationships. Volcanic rocks of the Punagarh and Sindreth Groups, for example, show well-preserved magmatic structures and textures; preliminary findings by members of our research team indicate that these rocks may be temporally and stratigraphically related to the Malani Igneous Suite rather than to the Delhi Supergroup (Van Lente, 2002), as suggested by Roy and Sharma (1999).

The extensive granitoid rocks that have been suggested, with variable degrees of confidence, to cut across the supracrustal rocks of the Delhi Supergroup, range in composition from true granite, to tonalite and diorite. These rocks, collectively referred to as Erinpura granites, are variably deformed, although at least some metamorphic fabric is present in most specimens. Age and geochemical

information is scant, and is mainly based on Rb–Sr whole-rock methods. In spite of these limitations, the available data indicate that the granitoids might comprise two or more age groupings. The extensive Mt. Abu granite, for example, has yielded an Rb–Sr age of 735 ± 15 Ma (Crawford, 1975), and if correct, this would imply an association with the ~750 Ma Malani Igneous Suite. Older Rb–Sr ages have been obtained for the Godhra (955 ± 20 Ma, Gopalan et al., 1979), Ambaji (~1228 Ma, Crawford, 1975), and Sendra (966 ± 250 Ma, Tobisch et al., 1994) granitoids, and dioritic rocks associated with metabasic rocks of the so-called Phulad Ophiolite yield an Sm–Nd whole rock age of 1012 ± 78 Ma (Volpe and Macdougall, 1990). Most recently, Deb et al. (2001) provided U–Pb zircon ages of 987 ± 6.4 and 986.3 ± 2.4 Ma for rhyolites in the Ambaji-Sendra 'arc terrane'. We report here the first U–Pb zircon age results for a possibly related granitic pluton of the Sendra Granitoid Suite, which is described below.

In the Sendra area (Figs. 1 and 2), there are five granitoid plutons ranging in size from 4 to ~15 km^2, and collectively referred to as the Sendra Granitoid Suite. Intrusive relationships with calc-silicate schists of the Delhi Supergroup (Sendra Formation, Kumbhalgarh Group) were documented by Agrawal and Srivastava (1997). Metamorphic fabrics are present in most of these granitoids (Tobisch et al., 1994), indicating syn-tectonic emplacement or the effects of a later deformational event, or both. Granitoids in most of these plutons are modally and chemically granodiorites or tonalites, although the largest of these, the Chang pluton, from which our samples were taken, is granitic in composition (Agrawal and Srivastava, 1997). Compositional and mineralogical details are presented and discussed below.

The only direct geochronological information for the Sendra granitoids comes from whole-rock Rb–Sr isotopic studies of Tobisch et al. (1994), which yield an imprecise

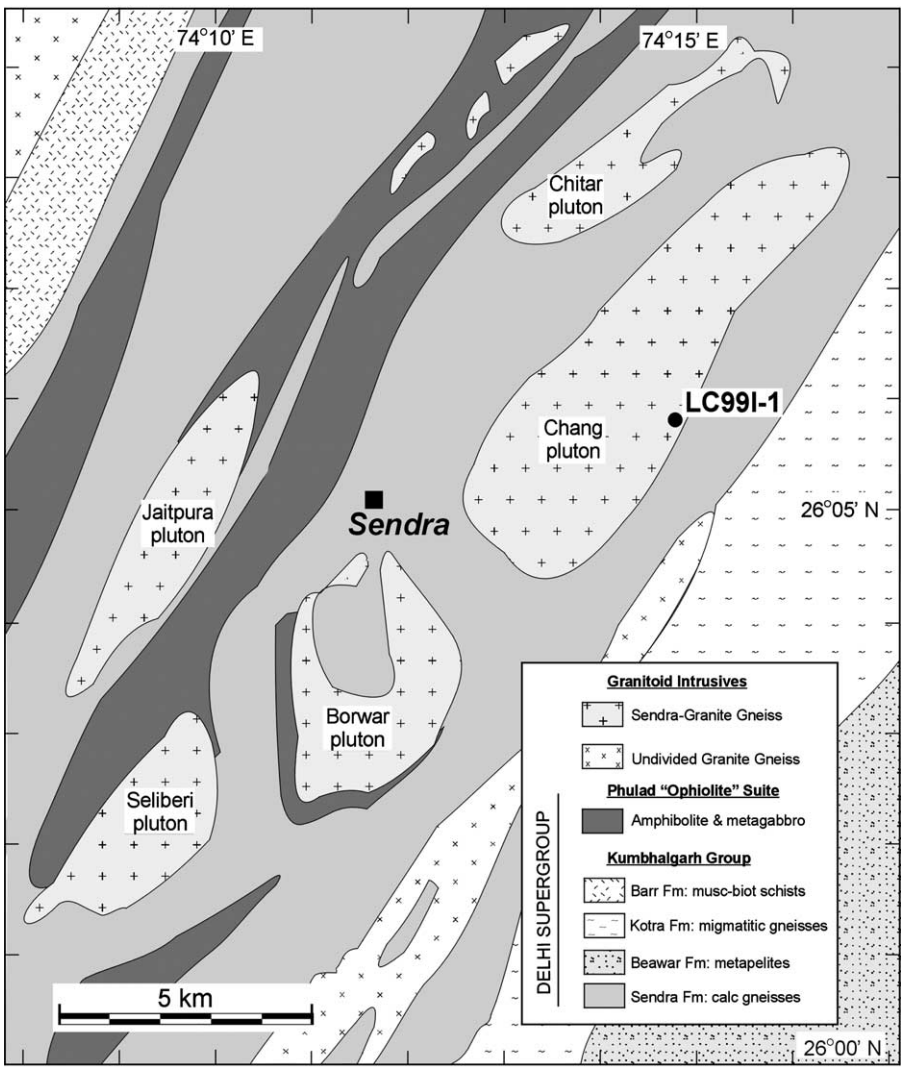

Fig. 2. Geological map of the Sendra region (adapted from Gupta et al., 1995) showing location of sampling site.

age of 966 ± 250 Ma, with initial $^{87}Sr/^{86}Sr$ (I_{Sr}) = 0.707 ± 0.034. Their samples were taken from the Chang and Seliberi plutons (Fig. 2), and from the (presumably related) Govindgarh pluton, which lies ~30 km NE of the main group of Sendra granitoid bodies. Tobisch et al. (1994) also presented Sm–Nd isotopic data for these rocks, which give T_{DM} model ages of 2.0–2.5 Ga, and $\varepsilon_{Nd,T}$ values of +2.2 to −6.9. Below we present additional chemical, Sr and Nd isotopic data that complement this work, in addition to U–Pb age determination and mineral compositions for granitoid rocks of the Chang pluton and for a spatially related metagabbro.

3. Sampling and analytical methods

Three specimens were collected from adjacent exposures in a single locality within the Chang pluton (Fig. 2, GPS coordinates: 26°5.8′N; 74°14.9′E). Sample LC99I-1A is a foliated biotite granite gneiss, typical of Chang pluton granitoids in this region. Also collected was a finer grained, more leucocratic, aplitic variety (LC99I-1B) that crosscuts sample 1A, and is interpreted as a late-magmatic dyke, although its thickness is indeterminate because only one of the contacts is exposed. Sample LC99I-1C is a massive, coarse grained (1–5 mm), hornblende-bearing metagabbro, collected from exposures within 100 m of samples LC99I-1A and 1B; contact relations with the adjacent granitoid rocks are obscured by loose blocks. The extent of this metagabbroic body is not known. It does not appear on available geological maps of the region. Petrographic, chemical, microprobe, and isotopic data are reported below for all three samples. Foliated granite LC99I-1A was selected for U–Pb zircon age determinations.

Major and trace element compositions were determined by standard X-ray fluorescence techniques as follows. Slabs representative of each whole-rock (generally >20 g) were trimmed of weathering rinds and powdered in a carbon steel vessel. For major elements, ~0.35 g of sample was mixed with ~2 g lithium tetraborate (Spectroflux), fused in a Pt/Au crucible for 2 h at 1000 °C, and cast into a glass bead. For trace elements, approximately 10 g of sample was compressed into a pellet. Analyses were carried out on Philips 1404 and X'Unique II instruments housed at the University of Natal, Durban, Department of Geology. Instrumental uncertainties are as follows: SiO_2, CaO, TiO_2, P_2O_5 (±0.2%); MgO (±0.3%); Al_2O_3, Fe_2O_3, MnO (±0.5%); Na_2O (±2%); Rb (±2%); Zr, Sr, Nb, Y (±3%); Zn, Cu, Ni, Cr, Ce, Nd (±5%); Sc, Pb, V, Ga, Co As, S (±10%); Ba, U, Th (±20%). Rare earth element (REE) concentrations were measured by ICP-AES at the Royal Holloway and Bedford New College, University of London, using Philips PV 8060 simultaneous/sequential optical ICP and Perkin–Elmer Optima 3300 radial ICP instruments. Details of analytical procedures can be found in Walsh et al. (1981) and Thompson and Walsh (1989). Major and trace element data are given in Table 1.

Quantitative energy-dispersive electron microprobe analyses were carried out on a Cameca Camebax instrument at Rand Afrikaans University. Operating conditions were: accelerating potential = 15kV, sample current = 10 nA (measured on brass), beam diameter = 1–2 μm. Standards included well-characterized natural silicate materials, and calculations were performed using a ZAF correction program. Representative mineral compositions and structural formulae are given in Table 2.

U–Pb zircon ages were determined by the isotope dilution method (Krogh, 1973), with modifications described in Tucker et al. (1998). Lead and uranium were loaded on single, outgassed Re filaments and analyzed in a VG Sector-54 mass spectrometer housed at Washington University, St. Louis, USA, using a single-collector procedure with a Daly photomultiplier detector operating in ion counting mode. In general, an ion beam between 0.5×10^{-14} and 6.5×10^{-13} A was maintained for ^{206}Pb during data acquisition and between 5.3×10^{-15} A and 3.0×10^{-14} for ^{235}U. Average total procedural blanks of 2 pg Pb and 0.2 pg U were maintained during the period of analysis; total common-Pb concentrations for all analyses are reported in Table 3. Initial-Pb corrections utilized the Pb isotopic composition estimated by Stacey and Kramers (1975) at the indicated age of the rock. In nearly all cases, the uncertainty in the amount of and composition of common-Pb calculated in this manner represents an insignificant contribution to the error of the calculated ages. Error propagation is similar to that developed by Ludwig (1980). Analytical reproducibility at 1σ confidence levels of replicate samples and standard solutions confirms that the parameters used in data reduction (see Table 3) and their errors have been evaluated correctly.

Samples for Rb–Sr and Sm–Nd isotopic analysis were cleaned and pulverized using standard techniques. Isotopic analyses were performed at the Mineralogical-Geological Museum, Oslo, Norway. Rb, Sr, Sm and Nd concentrations and isotopic ratios were determined by standard isotope dilution analytical methods, described in Knudsen et al. (1997), with VG 354 and Finnigan Mat 262 mass spectrometers. Nd isotopic compositions were normalized to $^{146}Nd/^{144}Nd = 0.7219$. During the period of analysis, the Johnson & Matthey Nd_2O_3 standard (batch no. S819093 A) yielded $^{143}Nd/^{144}Nd = 0.511101 \pm 13$ (2σ), and the NBS 987 Sr standard gave $^{87}Sr/^{86}Sr = 0.710190 \pm 50$ (2σ). Uncertainties in $^{147}Sm/^{144}Nd$ and $^{87}Rb/^{86}Sr$ are better than 0.25 and 0.5%, respectively. Rb–Sr isochron regressions were done using Isoplot/Ex (Ludwig, 1999), assuming blanket uncertainties (2σ) of 0.6% for $^{87}Rb/^{86}Sr$, and 0.01% for $^{87}Sr/^{86}Sr$. Rb–Sr and Sm–Nd concentration and isotopic data are given in Table 4. Note that as per convention,

Table 1
Major and trace element concentrations of Sendra granitoids and metagabbro

	Sample				
	LC99I-1A[a] biot. granite gneiss	LC99I-1B[a] aplitic leucogranite	Avg. Chang granite[b] $n = 20$	LC99I-1C[a] metagabbro	Avg. Phulad mafic[c] $n = 19$
SiO_2	76.57	77.80	73.18 ± 1.1	49.19	48.30 ± 1.5
TiO_2	0.16	0.08	0.13 ± 0.1	0.55	0.98 ± 0.5
Al_2O_3	12.00	12.11	14.42 ± 0.3	14.41	15.70 ± 1.6
$Fe_2O_3^T$	1.84	0.41	2.83 ± 0.5	10.80	11.79 ± 2.2
MnO	0.03	0.01	0.07 ± 0.01	0.19	0.18 ± 0.03
MgO	0.05	0.03	0.15 ± 0.1	9.15	9.18 ± 2.7
CaO	0.78	1.39	1.12 ± 0.4	13.13	11.65 ± 1.7
Na_2O	2.95	3.20	2.61 ± 0.2	1.69	1.64 ± 0.6
K_2O	5.01	4.57	4.57 ± 0.3	0.15	0.20 ± 0.2
P_2O_5	0.02	0.00	0.07 ± 0.03	0.04	0.12 ± 0.1
LOI	0.30	0.47		0.63	1.07 ± 0.26
	99.71	100.07	99.15	99.93	100.82
Trace elements in ppm					
Ba	502.4	117.2	627204	38.1	91125
V	4.5	1.3		230.8	23958
Cr	0	0	52	904.3	
Sc	4.1	0.6		70.5	
Co	153	152	61	79	
Ni	0.7	2.2	82	55.1	144120
Cu	0.2	1	62	9.6	
Zn	49.7	8.8	6915	73.6	
Ga	24	24		18	
Rb	330.2	274.5	24541	8.6	57
Pb	30	27			
Sr	37	111.3	4720	68.4	15292
Y	134	135.3		19.3	2510
Zr	205.3	131		21.7	6836
Nb	30.2	28.8		0.9	63
Th	37.6	50.1		0.5	
U	3.8	1.5		0.5	
S	151	0		4	
La	78.5	54.3		2.4	
Ce	156.15	107.07		6.18	
Pr	18.43	12.18		1.04	
Nd	73.08	46.81		5.07	9.45 ± 6.9
Sm	16.47	11.07		1.93	2.30 ± 1.2
Eu	1.63	0.55		0.79	
Gd	16.65	12.47		2.95	
Dy	20.72	18.35		3.86	
Ho	4.38	4.18		0.83	
Er	13.65	13.86		2.63	
Yb	14.73	15.97		2.46	
Lu	2.28	2.49		0.39	
CIPW norms, 100% anhydrous, FeO = 85% of Fe_{total}					
Q	37.85	39.21	36.84		
C	0.34		3.31		
Or	29.86	27.15	27.33	0.90	1.20
Ab	25.13	27.17	22.31	14.52	14.04
An	3.78	5.17	5.21	31.78	35.30
Di		0.95		27.85	18.37
Hy	2.34		4.04	16.58	21.03
Ol				5.06	5.55
Mt	0.36	0.07	0.56	2.17	2.36
Il	0.31	0.15	0.25	1.06	1.89
Ap	0.04	0.00	0.15	0.09	0.27

Table 1 (*continued*)

	Sample				
	LC99I-1A[a] biot. granite gneiss	LC99I-1B[a] aplitic leucogranite	Avg. Chang granite[b] $n = 20$	LC99I-1C[a] metagabbro	Avg. Phulad mafic[c] $n = 19$
	100.01	99.87	100.00	100.01	100.01
Norm An	13.08	15.99	18.93	68.64	71.54
Norm CI	3.01	1.17	4.85	52.72	49.20
Norm DI	92.84	93.53	86.48 ± 2.37	15.42	15.24
Al/(Na + Ca + K)	1.03	0.95	1.28 ± 0.07	0.54	0.65
K_2O/Na_2O	1.70	1.43	1.75 ± 0.18	0.09	0.12

Standard deviations are 1σ.
[a] Data from this study.
[b] Data from Agrawal and Srivastava (1997).
[c] Data from Volpe and Macdougall (1990).

uncertainties for U–Pb zircon data and ages are given to 1σ, whereas those for Rb–Sr and Sm–Nd are given to 2σ.

4. Results

4.1. Sample descriptions, petrography and mineralogy

Sample LC99I-1A is a grey, medium-grained (avg. grain size = 2–5 mm) biotite granite gneiss, with a prominent foliation formed by aligned biotite flakes and quartz-feldspar aggregates. Thin section examination reveals subequal proportions of quartz, plagioclase and microcline, about 3–5% brown biotite, with accessory muscovite, euhedral magnetite and apatite. Euhedral zircons up to 200 μm across, associated with biotite, are readily visible in thin sections. Plagioclase is unaltered, and shows normal and patchy zoning, ranging in composition from $An_{6.72}$ to $An_{13.98}$ (avg. = $An_{9.84\pm1.70}$, $n = 32$); coexisting microcline is unaltered and unexsolved, with uniform composition of $Or_{92.46-96.95}$ (avg. = $Or_{95.16\pm1.56}$, $n = 7$) (Table 2). Biotites are rich in annite component ($Fe^* = Fe/[Fe + Mg] = 0.901–0.923$), and show substantial Tschermak's substitution ($Al^{IV} = 2.413–2.561$, $n = 27$) (Table 2). The chlorine content of these biotites ranges from 0.38 to 0.50 wt% Cl (avg. = 0.49 ± 0.05, $n = 27$); these values are comparable to the highest of measured Cl contents in granitoid plutons of the Basin and Range Province, USA (Parry and Jacobs, 1975). We are unable to measure fluorine concentrations with our microprobe. Muscovite compositions are unremarkable, and show $Fe^* = 0.819–0.853$ (Table 2).

Sample LC99I-1B, which is interpreted as a dyke that cuts across the granitic gneiss typified by sample LC99I-1A, is a white to grey, medium to fine grained (avg. grain size = 0.5–1 mm) aplitic leucogranite with no more than 1–2% mafic minerals (biotite). Texturally, this rock consists of a granoblastic aggregate of quartz, plagioclase and microcline, with very minor equant aggregates of brown biotite and lesser muscovite. Fe–Ti oxides, apatite and zircon are not apparent in thin sections, but irregular monazite is a common accessory phase, texturally associated with biotite. Feldspars are unaltered, and show compositions nearly identical to the granite gneiss described above: plagioclase varies from $An_{2.89-19.20}$ (avg. = $An_{8.53\pm4.77}$, $n = 24$), and microcline is $Or_{92.97-98.28}$ (avg. = $Or_{94.88\pm1.13}$, $n = 21$). Biotites are compositionally similar to those of granite gneiss LC99I-1A, but with slightly lower Fe^* (0.856–0.872) and Cl (0.11–0.30 wt% Cl, avg. = 0.24 ± 0.05, $n = 16$), but with comparable Al^{IV} of 2.415–2.83 (Table 2). Muscovite compositions are also slightly lower in Fe^* (0.751–0.767) than those present in the granitoid gneiss (Table 2). Apart from these very minor differences, aplite LC99I-1B is mineralogically equivalent to granite gneiss LC99I-1A, but with finer grain size and lower colour index.

Sample LC99I-1C is a dark greenish, medium to coarse grained (avg. grain size = 3–5 mm) metagabbro, with massive texture and subequal proportions of dark green hornblende and grey to white plagioclase. In thin section, the rock consists of randomly oriented, elongate plagioclase crystals, some of which approach lath-like shapes, and aggregates of green to greenish-brown hornblende. Irregular grains of scapolite up to 3–4 mm across (66.3–73.2 meionite component, Table 2) are present in minor amounts; in some cases these contain euhedral needles of ferrian zoisite ($Fe^{3+}/[Fe^{3+} + Al] = 0.14–0.17$, Table 2) up to 1 mm long. The larger plagioclase grains in the rock (to 5–6 mm across) may be relict magmatic feldspars, and show strong normal compositional zoning. Most plagioclases, however, contain scattered secondary or metamorphic epidote or zoisite crystals 50–100 μm across, and amphibole needles 10–50 μm long. Microprobe analyses show that plagioclase composition varies widely, from $An_{44.85}$ to $An_{68.26}$ (avg. = $An_{61.39\pm5.65}$, $n = 35$). In part, the lower An contents are associated with later growth of epidote/zoisite. There is a clustering of amphibole compositions at magnesio-hornblende, although a few analyses vary toward actinolitic hornblende ($Fe/[Fe + Mg] = 0.341–0.397$;

Table 2
Representative microprobe analyses of Chang pluton samples

	Granite LC99I-1A				Aplite LC99I-1B				Metagabbro LC99I-1C			
	Plag	K-spar	Biotite	Musc	Plag	K-spar	Biotite	Musc	Plag	Hbld	Scapolite	Zoisite
SiO_2	64.67	64.09	34.82	46.86	66.25	63.89	35.34	47.45	51.11	47.56	47.55	38.35
TiO_2	n.a.	0.00	3.74	0.97	n.a.	0.00	2.23	0.18	n.a.	0.55	0.00	0.02
Al_2O_3	22.02	18.98	16.65	29.53	21.42	19.26	16.83	30.78	31.19	8.80	26.76	27.18
Cr_2O_3	n.a.	n.a.	0.04	0.06	n.a.	n.a.	0.12	0.00	n.a.	0.26	0.06	0.10
Fe_2O_3[a]											0.02	8.67
FeO[b]	0.22	0.00	29.84	6.78	0.00	0.32	29.44	5.82	0.00	14.35		
MnO	0.06	0.00	0.59	0.11	0.07	0.00	0.30	0.19	0.00	0.31	0.00	0.03
MgO	0.00	0.00	1.75	0.84	0.00	0.00	2.74	1.08	0.00	12.21	0.10	0.20
BaO	0.00	0.07	n.a.	n.a.	0.00	0.00	n.a.	n.a.	0.00	n.a.	n.a.	n.a.
CaO	2.14	0.00	0.00	0.00	1.28	0.00	0.00	0.00	12.97	11.98	15.96	23.28
ZnO	n.a.	n.a.	n.a.	n.a.	n.a.	n.a.	0.11	n.a.	n.a.	n.a.	n.a.	n.a.
Na_2O	10.62	0.67	0.66	0.25	11.42	0.54	0.29	0.22	4.42	1.02	4.38	0.10
K_2O	0.24	16.17	8.86	10.23	0.06	15.72	9.35	9.48	0.00	0.15	0.21	0.05
Cl	n.a.	n.a.	0.53	0.11	n.a.	n.a.	0.27	0.00	n.a.	0.06	0.74	0.00
	99.97	99.98	97.48	95.74	100.50	99.73	97.02	95.20	99.69	97.25	95.78	97.98
Structural formulae												
Basis	O = 8.0	O = 8.0	O = 22.0	O = 22.0	O = 8.0	O = 8.0	O = 22.0	O = 22.0	O = 8.0	O = 23.0	Si + Al = 12.0	O = 12.5
Si	2.854	2.968	5.507	6.393	2.897	2.960	5.585	6.424	2.329	7.005	7.214	2.994
Al	1.145	1.035	3.101	4.745	1.103	1.051	3.132	4.908	1.674	1.526	4.786	2.502
Ti		0.000	0.445	0.100		0.000	0.265	0.018		0.061	0.000	0.001
Cr			0.005	0.006			0.015	0.000		0.030	0.007	0.006
Fe^{3+a}											0.002	0.509
Fe^{2+b}	0.008	0.000	3.947	0.774	0.000	0.012	3.890	0.659	0.000	1.768		
Mn	0.002	0.000	0.079	0.013	0.003	0.000	0.040	0.022	0.000	0.039	0.000	0.002
Mg	0.000	0.000	0.413	0.171	0.000	0.000	0.645	0.218	0.000	2.681	0.023	0.023
Ba	0.000	0.001			0.000	0.000			0.000			
Ca	0.101	0.000	0.000	0.000	0.060	0.000	0.000	0.000	0.633	1.890	2.595	1.948
Zn							0.013					
Na	0.909	0.060	0.202	0.066	0.968	0.049	0.089	0.058	0.391	0.291	1.289	0.015
K	0.014	0.955	1.788	1.781	0.003	0.929	1.885	1.637	0.000	0.028	0.041	0.005
			Cl = 0.284	Cl = 0.051			Cl = 0.145				Cl = 0.190	
Total ions	5.033	5.020	15.487	14.049	5.034	5.001	15.559	13.944	5.027	15.319	16.146	8.005
Ab	88.77	5.91			93.89	5.01			38.18		Mol% Me	
An	9.86	0.00			5.82	0.00			61.82		66.3	
Or	1.37	94.09			0.29	94.99			0.00			
Fe/(Fe + Mg)[a]			0.910	0.820			0.858	0.751				
K/(Na + K)				0.964				0.966		0.397		

n.a. = not analysed.
[a] Total Fe as Fe_2O_3.
[b] Total Fe as FeO.

Table 3
U–Pb isotope dilution analyses, Chang pluton granitoid gneiss

Fractions		Concentrations					Atomic ratios				Age (Ma)
No.	Zircon properties[a]	Wt. (μg)[b]	Pb rad (ppm)[b]	U (ppm)[b]	Pb com (pg)[c]	Th/U[d]	$^{206}Pb/^{204}Pb$[e]	$^{207}Pb/^{206}Pb$[f]	$^{207}Pb/^{235}U$[f]	$^{206}Pb/^{238}U$[f]	$^{207}Pb/^{206}Pb$[f]
Chang pluton biotite granitoid gneiss (LC99I-1A)											
1	25 gr, cl, c, s-p	52	54.8	319	9.8	0.524	17, 287	0.07140 ± 3	1.5936 ± 41	0.16187 ± 42	968.9 ± 1.0
2	7gr, cl, c, s-p	12	59.6	350	5.3	0.509	8, 121	0.07133 ± 4	1.5814 ± 22	0.16080 ± 21	966.8 ± 1.1
3	7 gr, cl, c, s-p	13	42.8	256	2.2	0.487	14, 818	0.07135 ± 4	1.5627 ± 19	0.15885 ± 19	967.4 ± 1.2

[a] The first column denotes the number of the analysis as indicated in Fig. 5. The cardinal number in the second column indicates the number of zircon grains analysed (e.g. 7 gr = 7 grains). All analyses are of zircon from non-paramagnetic separates at 0° tilt at full magnetic field in Frantz Magnetic Separator; c = colourless; cl = clear; s-p = short-prismatic. All grains air-abraded following Krogh (1982).
[b] Concentrations are known to ~30% for sample weights of ~50 μg, and ~50% for samples of ~10 μg.
[c] Corrected for 0.0125 mole fraction common-Pb in the $^{205}Pb-^{238}U$ spike.
[d] Th concentration is calculated ($\lambda\ ^{232}Th = 4.9475 \times 10^{-11}\ y^{-1}$) from the excess ^{208}Pb after correction for introduced blank, common Pb and spike.
[e] Measured, uncorrected ratio.
[f] Ratio corrected for fractionation, spike, blank and initial common-Pb (at the determined age, from Stacey and Kramers, 1975). Pb fractionation correction = 0.094%/amu (±0.025%, 1σ); U fractionation correction = 0.111%/amu (±0.02%, 1σ). U blank = 0.2 pg; Pb blank ≤ 10 pg. Absolute uncertainties (1σ) in the Pb/U and $^{207}Pb/^{206}Pb$ ratios calculated following Ludwig (1980). $^{207}Pb/^{206}Pb$ age errors are 1σ. U and Pb half-lives and isotopic abundance ratios from Jaffey et al. (1971).

Si = 6.914–7.399 formula units per 23 oxygens, $n = 17$). Chlorine contents are low (0–0.11 wt% Cl).

4.2. Whole-rock major and trace element geochemistry

Chemical analyses of granitoids from the Chang pluton (Table 1) form a tight cluster of normative compositions in the monzogranite field (Fig. 3). Their leucocratic nature is demonstrated by their normative colour index values generally <5% (Table 1). Other plutons of the Sendra Granitoid Suite (Fig. 2) contain less potassic rocks, which classify as granodiorites and tonalities on a normative or modal basis (Fig. 3). In terms of alumina saturation, all Chang granitoids were stated to be peraluminous (Agrawal and Srivastava, 1997), although our two analysed samples straddle the boundary between peraluminous and metaluminous (Table 1).

Trace element concentrations of Chang granitoids show negative Ba, Nb, Sr, P and Ti anomalies on spider diagrams normalized to primordial mantle (Fig. 4a), as are typical of most granitoid rocks (e.g. Tarney and Jones, 1994). There are, however, noticeable enrichments in some incompatible elements (e.g. Pb, Rb, Th) relative to common granitoid types, at least for the two samples analysed. REE patterns for Chang pluton granitoids (Fig. 4b) show distinctive LREE as well as HREE enrichment, with La = 120–180 × chondrites, and Lu = 60–70 × chondrites, with conspicuous negative Eu anomalies ($[Eu/Eu^*]_N = 0.14–0.30$).

Metagabbro sample LC99I-1C has a basaltic composition, normatively equivalent to olivine tholeiite (Table 1). Major and trace element concentrations are quite comparable to many of the amphibolites and metagabbros of the Phulad 'Ophiolite' Suite, many of which have been suggested to have MORB-like characteristics (Volpe and Macdougall, 1990); the Chang metagabbro composition is equivalent to the mean of Phulad mafic rocks ($n = 19$) for all correspondingly analysed elements and oxides (Table 1). The REE pattern for the Chang metagabbro shows slight LREE-depletion, with no Eu anomaly, and abundances increasing smoothly from La = 5.4 × chondrites to Lu = 10.6 × chondrites (Fig. 4b). Concentrations of REE, Sr, Y, Zr and Nb for this sample are nearly identical (differing by a factor of <2–3) to those of average N-type MORB, compiled by Sun and McDonough (1989), although the metagabbro shows enrichments of up to 15 × N-MORB for Rb, U, Th and Ba. Similar enrichments in incompatible elements were observed for many Phulad mafic rocks by Volpe and Macdougall (1990).

4.3. Geochronology and isotopic systematics

Zircons separated from biotite granite gneiss LC99I-1A are optically clear, colourless, short, prismatic crystals that are free of inclusions. U–Pb isotopic data (Table 3) are plotted on a concordia diagram in Fig. 5. One of our analyses is concordant, two others are slightly discordant, and all three share a common $^{207}Pb/^{206}Pb$ age of 967.8 ± 1.2 Ma (1σ, MSWD = 1.12), which we interpret to represent the time of magmatic crystallization.

Rb–Sr whole-rock isotopic data for Sendra granitoids and metagabbro (data from this study and from Tobisch et al., 1994) are plotted in Fig. 6a. Results for the Chang pluton yield a regression of 906 ± 67 Ma (MSWD = 82, $n = 6$), with initial $^{87}Sr/^{86}Sr$ (I_{Sr}) = 0.718 ± 15. If data for granitoids from the spatially associated (and presumably coeval, Tobisch et al., 1994) Seliberi and Govindgarh plutons are included, a similar regression of 916 ± 48 Ma

Table 4
Rb–Sr and Sm–Nd isotopic data

Sample	Lithology	U–Pb age (Ma)[a]	Rb (ppm)	Sr (ppm)	$^{87}Rb/^{86}Sr$	$^{87}Sr/^{86}Sr$	I_{Sr} 968 Ma	Sm (ppm)	Nd (ppm)	$^{147}Sm/^{144}Nd$	$^{143}Nd/^{144}Nd$	ε_{Nd} 967 Ma[b]	T_{DM} (Ma)[b,c]
Chang pluton													
LC99I-1A[a]	Biot. granite gneiss	967.1 ± 1.6	340.98	38.46	26.5390	1.062951 ± 31	0.695638	17.476	77.682	0.1360	0.512097 ± 18	−3.041	1843
LC99I-1A (replicate)[a]			335.50					17.806	76.258	0.1411	0.512073 ± 12	−4.144	2025
LC99I-1B[a]	Aplitic leucogranite		264.32	105.33	7.3344	0.811744 ± 12	0.710232	11.801	48.651	0.1466	0.512154 ± 7	−3.243	2007
RAJ-12[d]	Biot. granite gneiss		223.8	52.14	12.6370	0.887372 ± 9	0.712470	21.05	102.30	0.1244	0.512039 ± 7	−2.734	1702
RAJ-12 (replicate)[d]	Biot. granite gneiss		227.0	52.20	12.8025	0.887040 ± 12	0.709847						
RAJ-11[d]			256.7	49.53	15.2950	0.912247 ± 13	0.700557	12.74	51.61	0.1492	0.512166 ± 16	−3.330	2060
RAJ-11(replicate)[d]			259.4	49.12	15.5875	0.914035 ± 9	0.698296	12.89	52.25	0.1491	0.512174 ± 16	−3.161	2038
LC99I-1C[a]	Metagabbro		5.32	73.16	0.2104	0.708687 ± 11	0.705775	1.938	5.258	0.2228	0.512952 ± 11	2.900	
Seliberi pluton													
RAJ-16[d]	Hbld-biot granodiorite		97.9	42.43	6.7351	0.798661 ± 9	0.705444	13.07	44.07	0.1793	0.512638 ± 5	2.161	1771
RAJ-16 (replicate)[d]	Hbld-biot granodiorite							13.05	43.95	0.1795	0.512652 ± 11	2.409	1718
Govindgarh pluton													
RAJ-29[d]			200.5	61.36	9.5788	0.842672 ± 22	0.710097	5.10	22.51	0.1369	0.511907 ± 16	−6.869	2247
Gneiss near Chang													
RAJ-3[d]	granitic gneiss		69.91	107.5	1.8851	0.726963 ± 9	0.7008722	6.2	21.6	0.1735	0.512485 ± 7	−0.110	2102

[a] Data from this study.
[b] Using CHUR parameters $^{147}Sm/^{144}Nd = 0.1967$, $^{143}Nd/^{144}Nd = 0.512368$.
[c] Using depleting mante model of DePaolo (1981).
[d] Data from Tobisch et al. (1994).

(MSWD = 102, $n = 8$), with initial $^{87}Sr/^{86}Sr$ (I_{Sr}) = 0.7153 ± 99 is obtained. Our new Rb–Sr isotopic data, therefore, improve the precision of the 966 ± 250 Ma age obtained by Tobisch et al. (1994), although the regressions are barely within error of the 967.8 ± 1.2 Ma U–Pb zircon age. Sm–Nd whole-rock isotopic data (Fig. 6b) do not yield meaningful age relationships for Chang pluton samples, or for any other combination of purportedly related rocks.

Initial Sr ratios calculated at the presumed crystallization age of 968 Ma ($I_{Sr\ 968}$) show a large variation for Chang pluton granitoids, from 0.69564 to 0.71247 (Table 4). Some of these $I_{Sr\ 968}$ values are impossibly low, especially for samples with high $^{87}Rb/^{86}Sr$, indicative of open system behaviour, as discussed below. Individual granitoid samples from the Seliberi (Fig. 2) and Govindgarh plutons yield $I_{Sr\ 968}$ values of 0.71010 and 0.70544, respectively (Tobisch et al., 1994), and metagabbro sample LC99I-1C has $I_{Sr\ 968}$ = 0.70578 (this study). Sm–Nd isotopic data for Chang pluton granitoids yield $\varepsilon_{Nd\ 968}$ values between −2.73 and −4.14 (mean $\varepsilon_{Nd\ 968} = -3.28 \pm 0.47$, $n = 6$). Individual samples from the Govindgarh ($\varepsilon_{Nd\ 968} = -6.87$) and Seliberi ($\varepsilon_{Nd\ 968} = +2.16$ to $+2.41$) plutons, as well as the Chang metagabbro ($\varepsilon_{Nd\ 968} = +2.90$) show Nd isotopic signatures that are distinctly different from each other, and from the Chang granitoids. The Nd isotopic evolution of Sendra samples is illustrated on diagrams of age vs. ε_{Nd} in Fig. 7. T_{DM} model ages of Sendra granitoids, calculated using the depleting mantle model of DePaolo (1981), range from 1.70 to 2.06 (Chang pluton), 1.72–1.77 (Seliberi pluton) and 2.25 Ga (Govindgarh pluton) (Table 4, Fig. 7a). The LREE-depleted Chang metagabbro has Sm/Nd > CHUR, and its Nd isotopic composition evolves toward higher ε_{Nd} values; similar Nd isotopic signatures are exhibited by many of the Phulad Suite mafic rocks (Fig. 7b).

5. Interpretation and discussion

5.1. Ages and Sr–Nd isotopic relations

Our U–Pb zircon result of 967.8 ± 1.2 Ma for the Chang pluton confirms, and substantially improves the precision of the crystallization age of the Sendra granitoids, that was previously constrained by a combined whole-rock Rb–Sr determination of 966 ± 250 Ma (Tobisch et al., 1994). The 967.8 ± 1.2 Ma crystallization age of the Chang pluton is equivalent, within error, to the Sm–Nd whole-rock regression of 1012 ± 78 Ma for the Ranakpur diorites (Volpe and Macdougall, 1990), some 150 km southwest of Sendra. These dioritic rocks have been suggested to be genetic relatives of the amphibolites and metagabbros of the Phulad Ophiolite (Volpe and Macdougall, 1990), some of which are chemically and isotopically similar to

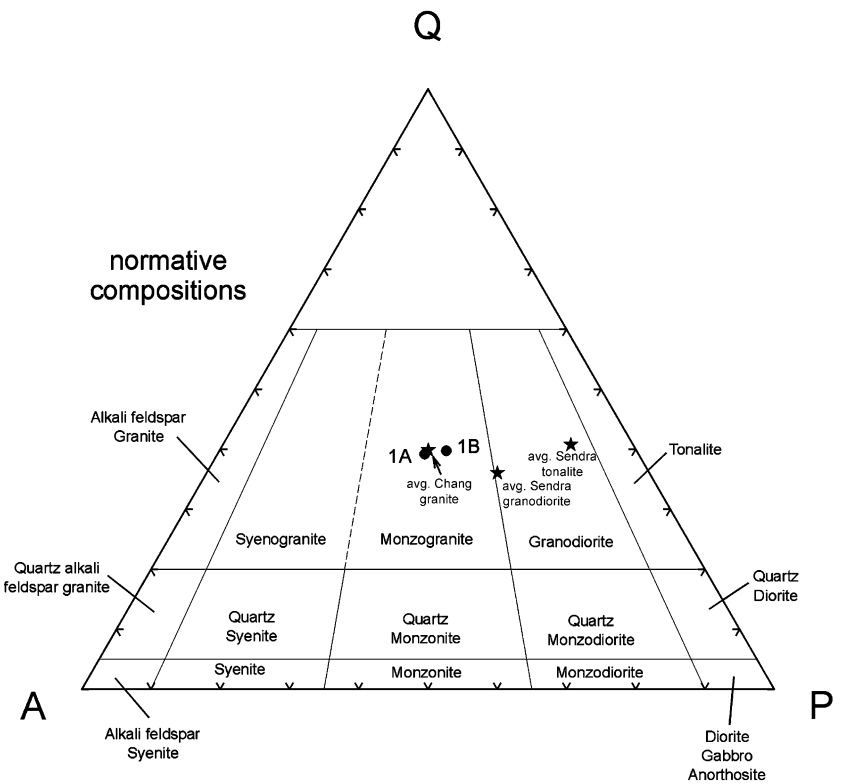

Fig. 3. Normative compositions of Sendra granitoid rocks, plotted on the classification diagram of Streckeisen (1976). Individual analyses of Chang pluton samples (1A, 1B, this study) are shown in comparison to averages (from Agrawal and Srivastava, 1997) of Chang granitoids ($n = 15$), and Sendra granodiorites ($n = 41$) and tonalites ($n = 12$).

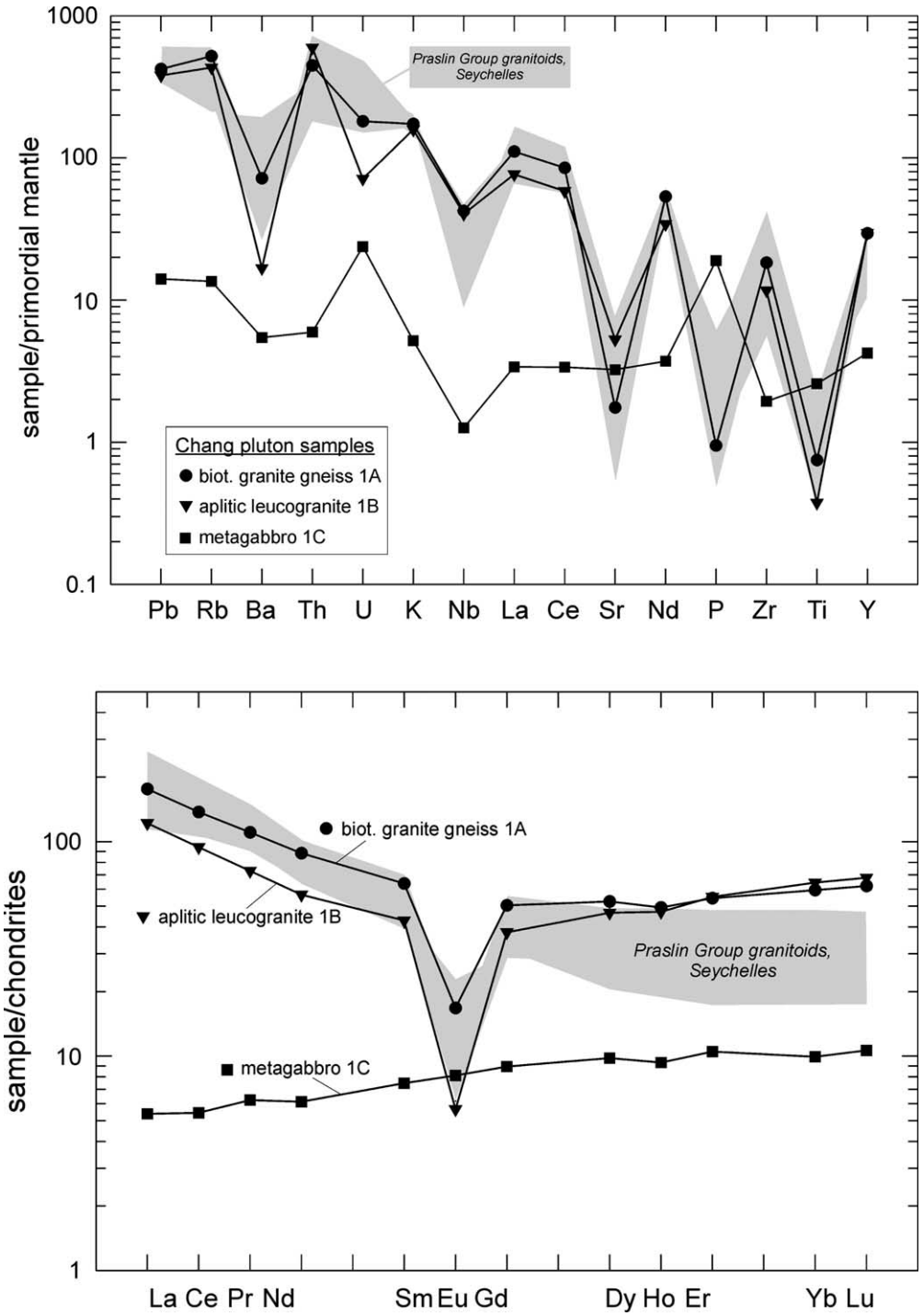

Fig. 4. (a). Normalized multi-element (spider) diagram comparing trace element patterns for Chang pluton granitoids (this study), with the field of Praslin Group granitoids of the Seychelles (Ashwal et al., 2002). Also shown are the data for a metagabbro sample associated with the Chang pluton. Data are normalized to 'primordial mantle' values of McDonough et al. (1992). (b). Chondrite-normalized REE plots comparing patterns for Chang granitoids (this study), with the field for Praslin Group granitoids of the Seychelles (Ashwal et al., 2002). The LREE-depleted pattern for metagabbro LC99I-1C is also shown. Chondritic abundances used are from Anders and Grevesse (1989).

the metagabbro we sampled at the Chang pluton. If these relationships are correct, one possible implication is that the Chang granitoids and metagabbro, as well as the extensive belt of metabasalts and metagabbros of the Phulad Suite were all coeval, although they have been variably affected by syn- and/or post-magmatic tectonothermal event(s). We stress however, that amongst Sendra granitoids and possible correlatives, only the Chang pluton is now well dated; further precise geochronology will be needed to establish whether or not other spatially associated plutonic entities

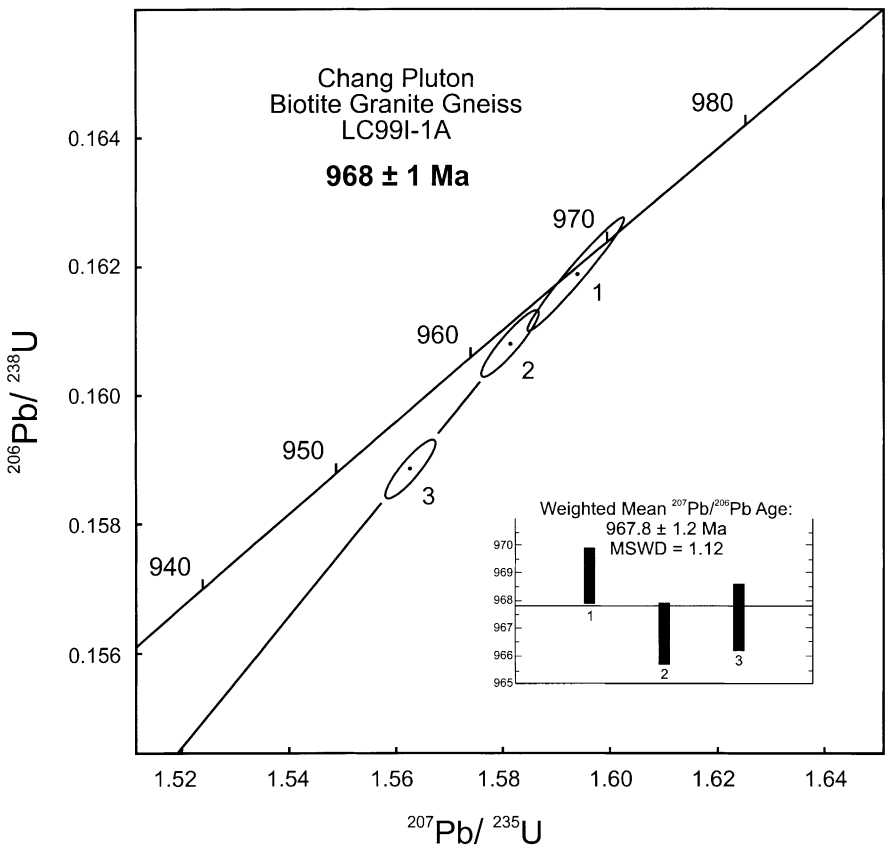

Fig. 5. Concordia diagram showing U–Pb zircon analyses for biotite granite gneiss LC99I-1A from the Chang pluton. Error ellipses for individual measurements represent analytical uncertainties at 1σ confidence levels. Numbers refer to individual analyses given in Table 3.

are coeval, and to constrain the time span of related magmatic activity.

Using our new whole-rock Rb–Sr data in combination with previous results of Tobisch et al. (1994) produces younger regressions of 916 ± 48 Ma (all Sendra granitoids) and 906 ± 67 Ma (Chang pluton only), which are barely within error of the 967.8 ± 1.2 Ma age of crystallization. We interpret this as indicative of at least some open system behaviour in the Rb–Sr whole-rock isotopic system, which is reflected in the impossibly low $I_{Sr\ 968}$ values of ~0.700 or less for those samples with high $^{87}Rb/^{86}Sr$ (by virtue of their low Sr concentrations of <50 ppm, Tables 1 and 4). Such features are common in granitoids (e.g. Cahen et al., 1976), and have recently been described by Ashwal et al. (2002) for ~750 Ma, undeformed granitoids of the Seychelles, in which the Rb–Sr whole rock isotopic system was proposed to have remained open to $^{87}Sr/^{86}Sr$ exchange, or was re-opened by a later heating event. Sr isotopic exchange is enhanced in rocks with low Sr concentration, and consequent high Rb/Sr, such as sample LC99I-1A (this study) and RAJ-11 (Tobisch et al., 1994) (Table 4). In the case of the Chang pluton, we cannot constrain whether Sr isotopic exchange took place between adjacent whole-rocks during protracted magmatic cooling of several to tens of m.y., or whether the Rb–Sr isotopic system was only partly equilibrated by a distinctly younger tectonothermal event. Of possible importance in this regard are three Sm–Nd mineral isochrons of 838 ± 36, 835 ± 43 and 791 ± 43 Ma, obtained for metagabbroic to dioritic rocks at Ranakpur (Fig. 1), and interpreted by Volpe and Macdougall (1990) as reflecting metamorphic re-equilibration during a ~800 Ma tectonomagmatic event. Again, careful geochronological work, preferably using multiple isotopic systems, is needed to resolve the post-magmatic metamorphic history of the Sendra granitoids in particular, and of the Aravalli Craton in general.

5.2. Constraints on possible magma sources

Open-system behaviour for some Chang pluton granitoids renders their magmatic I_{Sr} values subject to uncertainty, although the initial Nd isotopic ratios appear to be coherent. We estimate the initial magmatic isotopic compositions for Chang granitoids (based on simple means and 1σ standard deviations of values for samples presumed unaffected by open-system Sr effects, Table 4) to have been: $I_{Sr\ 968} = 0.7109 \pm 0.0014$ ($n = 3$), and $\varepsilon_{Nd\ 968} = -3.28 \pm 0.47$ ($n = 6$). Initial isotopic compositions for

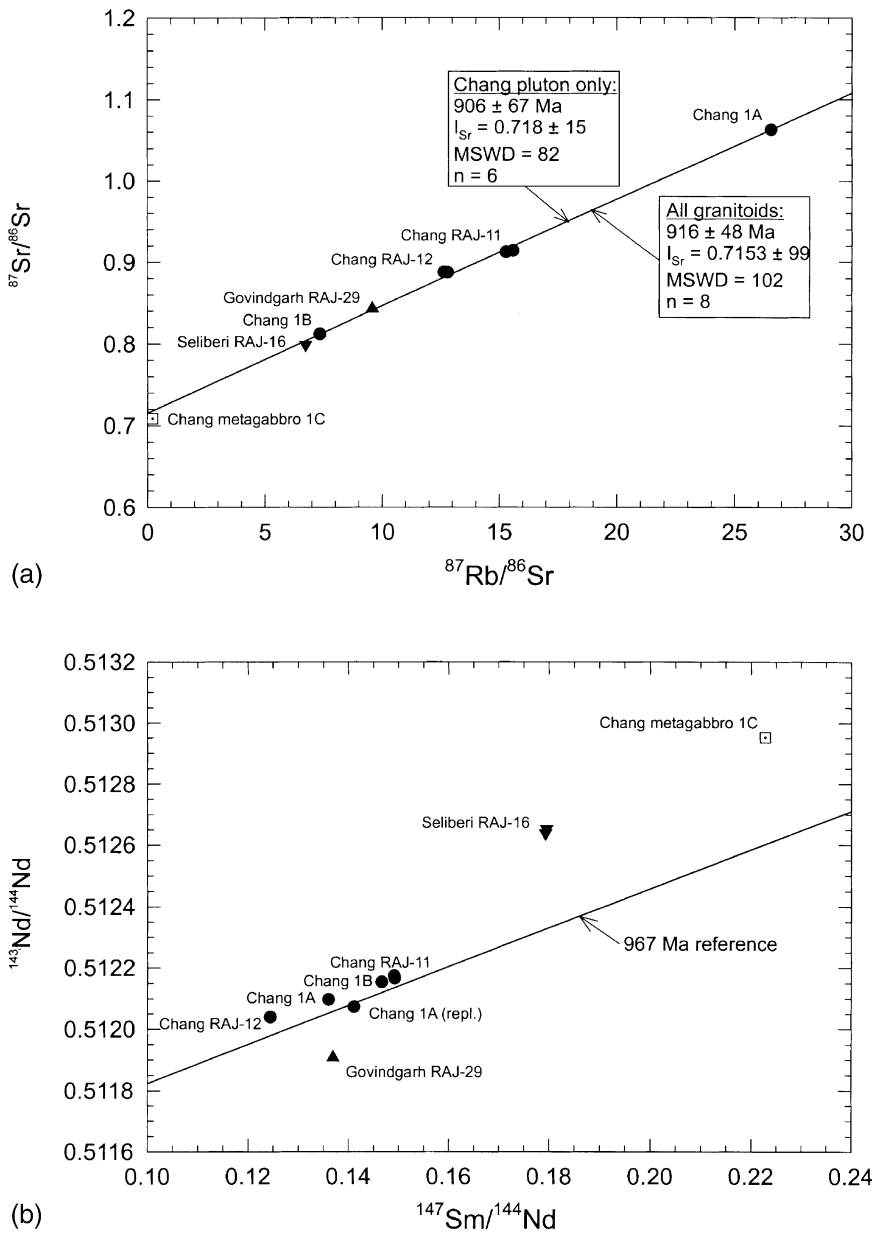

Fig. 6. Rb–Sr and Sm–Nd isochron diagrams for Sendra Suite granitoids from the Chang, Seliberi and Govindgarh plutons (filled symbols), and a metagabbro associated with the Chang pluton (open symbols). Data are from this study (LC99I-1A, 1B, 1C) and from Tobisch et al. (1994) (RAJ-11, 12, 16, 29). Maximum uncertainties in isotopic measurements are smaller than symbol sizes.

other Sendra granitoids, based on limited data (individual samples with and without replicate analyses, Tobisch et al., 1994, Table 4) are: $I_{Sr\ 968} = 0.7054$, $\varepsilon_{Nd\ 968} = +2.29 \pm 0.18$ (Seliberi pluton), and $I_{Sr\ 968} = 0.7101$, $\varepsilon_{Nd\ 968} = -6.87$ (Govindgarh pluton) (Figs. 7a and 8a).

Potential source materials for these granitoids include an assortment of older basement lithologies, many of which have not been studied in detail, and for which chemical and isotopic data are unavailable. Reasonably well-characterized candidates for possible sources of Sendra-type granitoids include Archaean rocks of the BGC, or the supracrustal sequences of the Palaeoproterozoic Aravalli Supergroup and Meso-to Neoproterozoic Delhi Supergroup. Of these, perhaps the best choices are the amphibolitic components of the BGC, whose age was estimated at 2.83 ± 0.05 Ga by Gopalan et al. (1990). These rocks, which include basaltic and basaltic andesite compositions, would have evolved by 968 Ma such that their Nd and Sr isotopic compositions would have overlapped those estimated for both the Chang and Govindgarh plutons (Figs. 7a and 8a). The ~3.3 Ga biotite gneisses of the BGC would have had Nd and Sr isotopic compositions far too radiogenic at 968 Ma to represent viable sources for Sendra-type granitoids (Figs. 7a and 8a). A single granodiorite (and replicate) from the Seliberi pluton (Fig. 8) has more primitive initial Nd and Sr isotopic signatures that lie

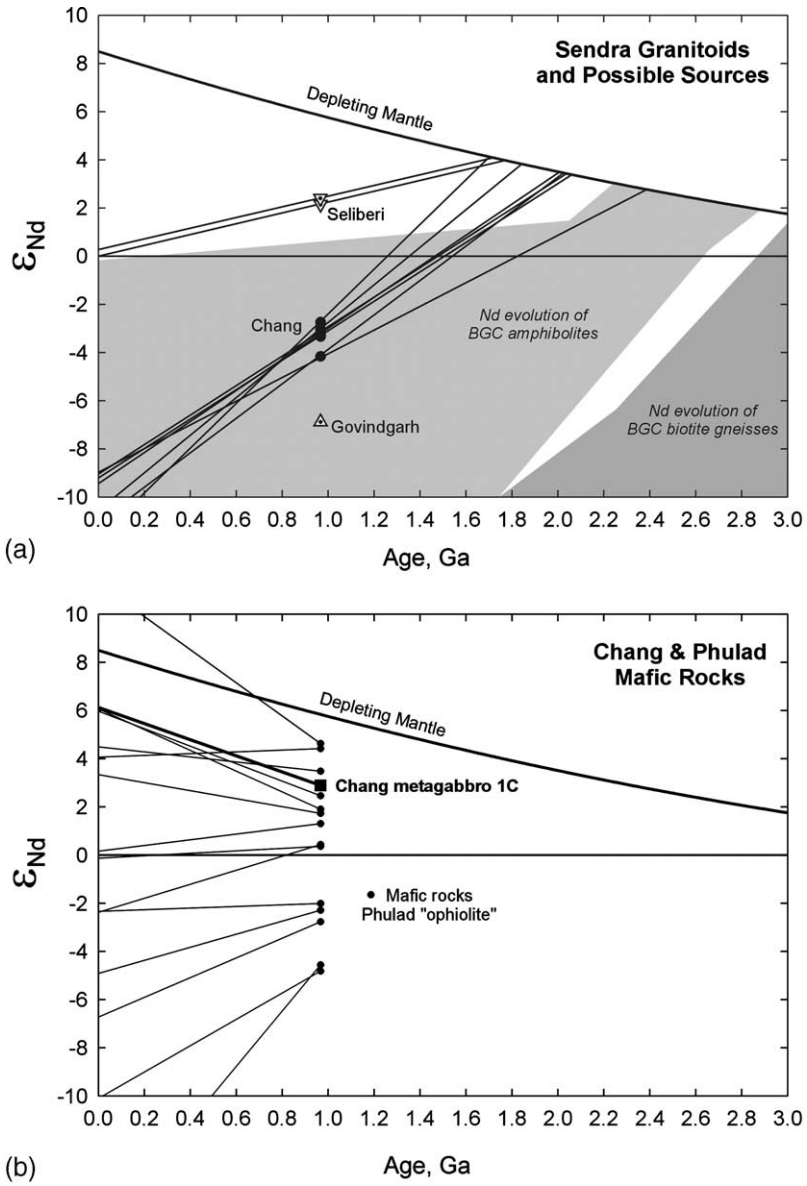

Fig. 7. Plots of age vs. epsilon Nd, showing Nd isotopic evolution of for individual samples. Depleting mantle curve is from DePaolo (1981). (a) Granitoid rocks from the Chang, Seliberi and Govindgarh plutons (data from this study and Tobisch et al., 1994) are compared with fields showing the Nd isotopic evolution of Archaean amphibolites and biotite gneisses of the BGC (data from Gopalan et al., 1990 and Tobisch et al., 1990). (b) Nd isotopic evolution of individual mafic rocks, including the Chang metagabbro (this study) and those of the Phulad 'ophiolite' suite (Volpe and Macdougall, 1990).

outside the evolution field of BGC amphibolites. This could indicate the presence of a mantle-derived and/or juvenile component in the Seliberi source or parental magma; alternatively, and perhaps more likely, is that the 9 samples of Archaean BGC amphibolite analysed by Gopalan et al. (1990) do not represent the entire spectrum of isotopic compositions present.

Partial melting of BGC amphibolites can be reasonably expected to yield magma compositions similar to the tonalites and granodiorites of the Govindgarh, Seliberi and other Sendra-type plutons. It seems less likely, however, for the (monzo)granitic compositions (Fig. 3) of the Chang pluton to have been generated in this way. Distinct differences in Nd and Sr isotopic compositions (Figs. 7a and 8a) further preclude the possibility that Sendra-type plutons could be related by simple fractional crystallization, a conclusion reached by Agrawal and Srivastava (1997) on the basis of major element chemistry. A mixed source seems more likely, with each of the Sendra plutons having been generated by partial melting, for example, of variable proportions of BGC amphibolites, BGC biotite gneisses, and possibly one or more younger source components. Further geochemical and isotopic work on both Sendra granitoids as well as potential source materials will be needed to resolve this.

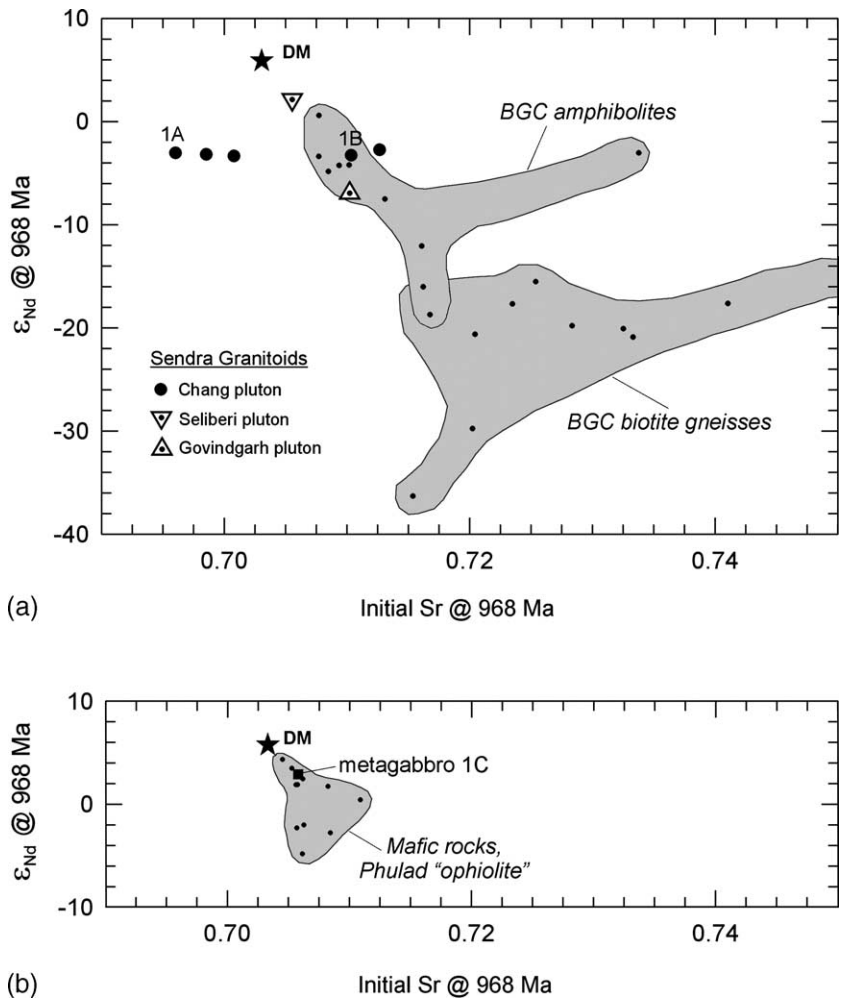

Fig. 8. Plots of initial Sr vs. epsilon Nd (both calculated at 968 Ma), for Sendra Suite magmatic rocks and possible source materials. Approximate composition of depleted mantle (DM) at 968 Ma is calculated from estimates given by DePaolo (1981) and DePaolo and Wasserburg (1976). (a) Granitoid rocks from the Chang, Seliberi and Govindgarh plutons (data from this study and Tobisch et al., 1994) are compared with fields showing the Sr and Nd isotopic compositions (at 968 Ma) of Archaean amphibolites and biotite gneisses of the BGC (data from Gopalan et al., 1990 and Tobisch et al., 1994). (b) Chang metagabbro LC99I-1C (this study) is compared with the field for mafic rocks of the Phulad ophiolite suite (Volpe and Macdougall, 1990).

The Chang metagabbro has Nd ($\varepsilon_{Nd\ 968} = +2.90$) and Sr ($I_{Sr\ 968} = 0.7058$) isotopic signatures that approach, but are not as primitive as model depleted mantle (DM) at 968 Ma ($\varepsilon_{Nd\ DM\ 968} = +5.83$, $I_{Sr\ DM\ 968} = 0.70334$, DePaolo, 1981; DePaolo and Wasserburg, 1976) (Figs. 7b and 8b). Crustal contamination seems unlikely to account for the higher $I_{Sr\ 968}$ and lower $\varepsilon_{Nd\ 968}$ in the metagabbro relative to DM, given its low LILE concentrations (Fig. 4a), LREE-depleted signature (Fig. 4b) and overall MORB-like chemistry (Table 1). Therefore, derivation from a source slightly less depleted (lower Sm/Nd) than model DM seems likely, a conclusion also reached on this basis by Volpe and Macdougall (1990) for some of the Phulad Suite metabasalts and metagabbros.

5.3. Petrologic relations

The only significant chemical differences among our studied granitoid samples from the Chang pluton relate to a slight enrichment in mafic constituents (principally Fe) in biotite granite gneiss LC99I-1A relative to leucogranite LC99I-1B (Table 1). Otherwise, the two samples are chemically similar in terms of major, minor and trace elements. This is illustrated by the coherence of their trace element (Fig. 4a) and REE patterns (Fig. 4b), as well as their normative abundances (Fig. 3). Compositions of plagioclase, K-feldspar, biotite and muscovite are effectively identical in the two samples (Table 2). These features, coupled with their Sr and Nd isotopic compositions, suggest to us that the two samples are coeval and comagmatic components of a single granitoid pluton, with leucogranite LC99I-1B representing a late-magmatic dyke.

We cannot account for the apparent discrepancy in alumina saturation between our XRF whole-rock data, and the average of 20 Chang granitoids (Agrawal and Srivastava, 1997), determined by atomic absorption spectrophotometry (Table 1). The peraluminous (as indicated by their data) vs. metaluminous (as indicated by ours) character of

the Chang granitoids is important, especially in considering the properties of possible source materials. It seems unlikely that a mixed source dominated by amphibolite and tonalitic gneiss, as discussed above, would yield peraluminous granitoid magmas, which are generally perceived as indicative of metasedimentary-dominated sources (so-called 'S-type granites' of Chappell and White, 1974). Until the peraluminous chemistry of Chang granitoids can be demonstrated by re-analysis, we maintain that their metaluminous character, as indicated by our data, is best interpreted in terms of 'I-type' classification and source characteristics.

In this regard, we consider the presence of accessory muscovite (Table 2) and garnet (Agrawal and Srivastava, 1997; Tobisch et al., 1994) in some Chang granitoids as metamorphic in origin, rather than reflective of peraluminous rock chemistry. The minor K-rich muscovites present in our Chang samples may, in fact, represent recrystallized products of sericitic feldspar alteration, produced during late-magmatic hydrothermal processes. This would account for the chemical similarities between granitoids of the Chang pluton, and those of the Praslin Group (Seychelles), for which an imparted hydrothermal signature has been recently proposed by Ashwal et al. (2002) to account for their LILE enrichment.

Despite having been reconstituted under metamorphic conditions similar to those of Chang granitoids (low-mid amphibolite facies), metagabbro sample LC99I-1C appears to have retained magmatic chemistry, including a LREE-depleted signature ($[La/Sm]_N = 0.72$), low K content (1245 ppm) and many other element ratios that are well within the range of MORB compositions, taken from numerous compilations of data (e.g. Basaltic Volcanism Study Project, 1981; Sun et al., 1979). Given these properties, the composition of the Chang metagabbro may approach that of a magmatic liquid, although its texture suggests that its precursor was probably a medium-to coarse-grained gabbro rather than a basaltic volcanic rock. Volpe and Macdougall (1990) argued against magmatic assimilation of continental crustal components by the precursors to the Phulad Suite mafic rocks, with which our metagabbro sample is likely related. Rather, the slight enrichments in some LILE relative to MORB were attributed to fluid exchange processes during regional metamorphism. Our data are compatible with this, and the secondary scapolite and ferrian zoisite in our sample may have precipitated from metamorphic fluids that interacted with the carbonate-rich units of the surrounding Delhi Supergroup. We suggest that such effects may be responsible, in part, for the elevated Rb (8.6 ppm), Ba (38.1 ppm) U (0.5 ppm) and Th (0.5 ppm) in LC99I-1C relative to average N-MORB (Rb = 0.56 ppm, Ba = 6.3 ppm, U = 0.047 ppm, Th = 0.12 ppm; Sun and McDonough, 1989). Other chemical attributes of this sample, including Sr and Nd isotopic compositions, were largely unaffected by metamorphic processes.

5.4. Local and regional correlations and implications

The 968 Ma emplacement age of the Chang pluton leads to the obvious consideration of the abundance and spatial extent of ca. 1 Ga magmatic rocks in Rajasthan, and possible correlatives with other ca. 1 Ga equivalents elsewhere. We conclude, based on the available data, that the other spatially associated granitoid plutons of the Sendra group (Fig. 2) are likely to be coeval with Chang, although precise geochronology is needed to confirm this, and to establish the actual time span of magmatic activity. Other entities in the Aravalli Craton that are also possibly coeval include the mafic and related rocks of the Phulad Ophiolite Suite, and the Erinpura granites (Fig. 1). If future geochronological work establishes a temporal connection between these rocks, then a substantial belt of ca. 1 Ga metaigneous rocks will have been identified. Our results are compatible with a convergent margin setting, with the Chang and related granitoid plutons representing Andean-type plutons; the mafic rocks of the Phulad Suite as well as the metagabbro studied in this paper may represent contemporary ocean floor and/or arc-related magmatic products, as in the ophiolite model of Volpe and Macdougall (1990). Confirmation of such a model would have important implications for currently debated issues relevant to Late Precambrian continental evolution, such as the construction of the Rodinia supercontinent at ~1 Ga (e.g. Weil et al., 1998).

Magmatic rocks with ages of ~1 Ga are increasingly being identified in other continental fragments that may have lain in close proximity to northwestern India during the Late Precambrian. For example, in the central part of Madagascar, whose position adjacent to Rajasthan at ~750 Ma (and probably earlier) has been discussed by Torsvik et al. (2001), intrusions of granodioritic (Dabolava pluton, 1002 ± 3 Ma) and gabbroic (Miandrivazo pluton, 982 ± 2 Ma) composition have recently been described (Rakotoarimanana et al., 2000). The granodiorites are associated with quartz vein-hosted gold deposits that are presently exploited by local artisans; if this mineralization is temporally restricted to ~1 Ga granitoids, a significant exploration tool may emerge. The existence of a ~1 Ga belt of magmatic rocks would also have significant implications for Rodinia reconstructions. Kröner et al. (2000), for example, have highlighted the apparent *absence* of ca. 1 Ga magmatic and metamorphic rocks in Madagascar, leading to their speculation that Madagascar may have been attached to eastern Africa rather than western India at this time, or that it formed a separate microcontinent. We expect that further work of the kind reported in this paper will contribute toward a deeper understanding of these issues, which may have economic as well as academic significance.

Acknowledgements

Funds to support this work were supplied by the DST, India (Grant ESS/023/015), the Norwegian Research Council, the National Science Foundation (USA) and the National Research Foundation (South Africa). We thank Dr S.K. Acharyya, Director General, Geological Survey of India, for providing logistical support for fieldwork. The authors are indebted to Tom Andersen (Mineralogical-Geological Museum, Oslo), who provided access to his lab, and assistance with the Sr and Nd isotopic analyses. Belinda Van Lente, Sergio Mkaza and Nellie Day (Rand Afrikaans University) helped with the microprobe analyses, and the XRF data were expertly obtained by Roy Seyambu (University of Natal, Durban). Roberta Galba Brasilino (Federal University of Pernambuco, Recife) is thanked for assistance in compilation of the geological maps. John Tarney and Michael Wiedenbeck supplied helpful comments on an earlier version of the manuscript.

References

Agrawal, S., Srivastava, R.K., 1997. Geochemistry of Late Proterozoic Sendra granitoid suite, central Rajasthan, India: role of magma mixing/hybridization process in their genesis. J. Geol. Soc. India 50, 607–618.

Ahmad, T., Tarney, J., 1994. Geochemistry and petrogenesis of late Archaean Aravalli volcanics, basement enclaves and granitoids, Rajasthan. Precamb. Res. 65, 1–23.

Anders, E., Grevesse, N., 1989. Abundances of the elements: meteoritic and solar. Geochim. Cosmochim. Acta 53, 197–214.

Ashwal, L.D., Demaiffe, D., Torsvik, T.H., 2002. Petrogenesis of Neoproterozoic granitoids and related rocks from the Seychelles: the case for an Andean-type arc origin. J. Petrol. 43, 45–83.

Basaltic Volcanism Study Project, 1981. Basaltic Volcanism on the Terrestrial Planets, Pergamon Press, New York, 1286 pp.

Bhushan, S.K., 2000. Malani rhyolites—a review. Gondwana Res. 3, 65–77.

Bose, U., 1989. Correlation problems of the Proterozoic stratigraphy of Rajasthan. Indian Mineral. 43, 183–193.

Cahen, L., Delhal, J., Ledent, D., 1976. Chronologie de l'orogenèse Ouest-Congolienne (Pan Africaine) et comportement isotopique de roches d'alcalinite différente dans la zone interne de l'orogène, au Bas-Zaire. Annal. Soc, Géol. Belgique 99, 189–203.

Chappell, B.W., White, A.J.R., 1974. Two contrasting granite types. Pacific Geol. 8, 173–174.

Choudhary, A.K., Gopalan, K., Sastry, C.A., 1984. Present status of the geochronology of the Precambrian rocks of Rajasthan. Tectonophysics 105, 131–140.

Coulson, A.L., 1933. The geology of Sirohi state, Rajputana. Mem. Geol. Surv. India 63, 166.

Crawford, A.R., 1975. Rb–Sr age determination for the Mount Abu granite and related rocks of Gujarat. J. Geol. Soc. India 16, 20–28.

Crawford, A.R., Compston, W., 1970. The age of the Vindhyan system of peninsular India. Quart. J. Geol. Soc. Lond. 125, 351–372.

Deb, M., Thorpe, R.I., Krstic, D., Corfu, F., Davis, D.W., 2001. Zircon U–Pb and galena Pb isotope evidence for an approximate 1.0 Ga terrane constituting the western margin of the Aravalli–Delhi orogenic belt, northwestern India. Precamb. Res. 108, 195–213.

DePaolo, D.J., 1981. Neodymium isotopes in the Colorado Front Range and crust-mantle evolution in the Proterozoic. Nature 291, 193–196.

DePaolo, D.J., Wasserburg, G.J., 1976. Inferences about magma sources and mantle structure from variations of $^{143}Nd/^{144}Nd$. Geophys. Res. Lett. 3, 743–746.

Gopalan, K., Trivedi, J.R., Merh, S.S., Patel, P.P., Patel, S.G., 1979. Rb–Sr age of Godhra and related granites, Gujarat, India. Proc. Indian Acad. Sci. 108, 60–68.

Gopalan, K., Macdougall, J.D., Roy, A.B., Murali, A.V., 1990. Sm–Nd evidence for 3.3 Ga old rocks in Rajasthan, northwestern India. Precamb. Res. 48, 287–297.

Gupta, B.C., 1934. The geology of central Mewar. Mem. Geol. Surv. India 65, 107–168.

Gupta, B.C., Mukherjee, P.N., 1938. Geology of Gujarat and southern Rajputana. Rec. Geol. Surv. India 73, 163–208.

Gupta, S.N., Arora, Y.K., Mathur, R.K., Iqbaluddin, B.P., Prasad, B., Sahai, T.N., Sharma, S.B., 1995. Geological map of the Precambrians of the Aravalli region, southern Rajasthan and northwestern Gujarat, India (4 sheets, scale 1:250,000). Geol. Surv. India, Western Region, Jaipur, India.

Gupta, S.N., Arora, Y.K., Mathur, R.K., Iqbaluddin, B.P., Prasad, B., Sahai, T.N., Sharma, S.B., 1997. The Precambrian geology of the Aravalli region, southern Rajasthan and northeastern Gujarat. Mem. Geol. Surv. India 123, 262.

Heron, A.M., 1917. Geology of north-eastern Rajputana and adjacent districts. Mem. Geol. Surv. India 45, 128.

Heron, A.M., 1953. The geology of central Rajputana. Mem. Geol. Surv. India 79, 389.

Jaffey, A.H., Flynn, K.F., Glendinin, L.E., Beltley, W.C., Essling, A.M., 1971. Precision measurement of half-lives and specific activities of ^{235}U and ^{238}U. Phys. Rev. C 4, 1889–1906.

Knudsen, T.-L., Andersen, T., Maijer, C., Verschure, R.H., 1997. Trace-element characteristics and Pb isotopic evolution of metasediments and associated Proterozoic rocks from the amphibolite- to granulite-facies Bamble sector, southern Norway. Chem. Geol. 143, 145–169.

Krogh, T.E., 1973. A low-contamination method for hydrothermal decomposition of zircon and extraction of U and Pb for isotopic age determinations. Geochim. Cosmochim. Acta 37, 485–494.

Krogh, T.E., 1982. Improved accuracy of U–Pb zircon dating by the creation of more concordant systems using air abrasion technique. Geochim. Cosmochim. Acta 46, 637–649.

Kröner, A., Hegner, E., Collins, A.S., Windley, B.F., Brewer, T.S., Razakamanana, T., Pidgeon, R.T., 2000. Age and magmatic history of the Antananarivo block, central Madagascar, as derived from zircon geochronology and Nd isotopic systematics. Am. J. Sci. 300, 251–288.

Ludwig, K.R., 1980. Calculation of uncertainties of U–Pb isotopic data. Earth Planet. Sci. Lett. 46, 212–220.

Ludwig, K.R., 1999. User's manual for Isoplot/Ex version 2.3, Berkeley Geochronology Center Special Publication 1a, Berkeley Geochronology Center, Berkeley CA, 53 pp

McDonough, W.F., Sun, S.-S., Ringwood, A.E., Jagoutz, E., Hoffmann, A.F., 1992. Potassium, rubidium and cesium in the Earth and Moon and the evolution of the mantle of the Earth. Geochim. Cosmochim. Acta 56, 1001–1012.

Naha, K., Halyburton, R.V., 1974. Early Precambrian stratigraphy of central and southern Rajasthan, India. Precamb. Res. 1, 55–73.

Naha, K., Roy, A.B., 1983. The problem of the Precambrian basement in Rajasthan, western India. Precamb. Res. 19, 217–223.

Pareek, H.S., 1981. Petrochemistry and petrogenesis of the Malani igneous suite, India. Summary. Geol. Soc. Am. Bull. 92, 62–70.

Parry, W.T., Jacobs, D.C., 1975. Fluorine and chlorine in biotite from Basin and Range plutons. Econ. Geol. 70, 554–558.

Rakotoarimanana, R.H., Ashwal, L.D., Robb, L.J., Tucker, R.D., 2000. Quartz vein hosted gold mineralisation in Proterozoic dioritic plutons within the Dabolava metavolcanic complex, west Madagascar (abstr). Geol. Soc. S. Afr. Geocongress 2000, Stellenbosch, J. Afr. Earth Sci. 31, 59.

Roy, A.B., Kataria, P., 1999. Precambrian geology of Aravalli Mountains and neighborhood-analytical update of recent studies. In: Kataria, P., (Ed.), Proceedings of the Seminar on the Geology of Rajasthan: Status and Perspective, MLS University, Udaipur, pp. 1–56.

Roy, A.B., Kröner, A., 1996. Single zircon evaporation ages constraining the growth of the Archaean Aravalli craton, northwest Indian shield. Geol. Mag. 133, 333–342.

Roy, A.B., Sharma, K.K., 1999. Geology of the region around Sirohi town, western Rajasthan—a story of Neoproterozoic evolution of the Aravalli crust. In: Paliwal, B.S., (Ed.), Evolution of Northwestern India, Scientific Publishers, Jodhpur, pp. 19–33.

Roy, A.B., Paliwal, B.S., Shekhawat, S.S., Nagori, D.K., Golani, P.R., Bejarniya, B.R., 1988. Stratigraphy of the Aravalli Supergroup in the type area. Geol. Surv. India Mem. 7, 121–138.

Sharma, R.S., 1995. An evolutionary model for the Precambrian crust of Rajasthan: some petrological and geochronological considerations. Mem. Geol. Soc. India 31, 91–115.

Sinha Roy, S., Malhotra, G., Mohanty, M., 1998. Geology of Rajasthan, Geological Society of India, Bangalore, 278 pp.

Stacey, J.S., Kramers, J.D., 1975. Approximation of terrestrial lead isotope evolution by a two-stage model. Earth Planet. Sci. Lett. 26, 207–221.

Streckeisen, A., 1976. To each plutonic rock its proper name. Earth Sci. Rev. 12, 1–33.

Sugden, T.J., Deb, M., Windley, B.F., 1990. Tectonic setting of mineralization in the Proterozoic Aravalli–Delhi orogenic belt. In: Naqvi, S.M., (Ed.), Precambrian Continental Crust and its Economic Resources, Developments in Precambrian Geology, vol. 8. Elsevier, Amsterdam, pp. 367–390.

Sun, S.-S., McDonough, W.F., 1989. Chemical and isotopic systematics of oceanic basalts: implications for mantle composition and processes. Geol. Soc. Lond. Spec. Publ. 42, 313–345.

Sun, S.-S., Nesbitt, R.W., Sharaskin, A.Y., 1979. Geochemical characteristics of mid-ocean ridge basalts. Earth Planet. Sci. Lett. 44, 119–138.

Tarney, J., Jones, C.E., 1994. Trace elements geochemistry of orogenic igneous rocks and crustal growth models. J. Geol. Soc. Lond. 151, 855–868.

Thompson, M., Walsh, J.N., 1989. A Handbook of ICP Spectrometry, Second ed, Blackie, Glasgow, 316 pp.

Tobisch, O.T., Collerson, K.D., Bhattacharyya, T., Mukhopadhyay, D., 1994. Structural relationship and Sr–Nd systematics of polymetamorphic granitic gneisses and granitic rocks from central Rajasthan, India: implications for the evolution of the Aravalli craton. Precamb. Res. 65, 319–339.

Torsvik, T.H., Carter, L.M., Ashwal, L.D., Bhushan, S.K., Pandit, M.K., Jamtveit, B., 2001. Rodinia refined or obscured: palaeomagnetism of the Malani Igneous Suite (NW India). Precamb. Res. 108, 319–333.

Tucker, R.D., Bradley, D.C., Ver Staeten, C.A., Harris, A.G., Ebert, J.R., McCutcheon, S.R., 1998. New U–Pb zircon ages and the duration and division of Devonian time. Earth Planet. Sci. Lett. 158, 175–186.

Van Lente, B., 2002. Petrology, geochemistry and geochronology of Neoproterozoic volcanic rocks of the Punagarh and Sindreth Groups, Rajasthan, northwest India. MSc thesis, Rand Afrikaans University, Johannesburg

Volpe, A.M., Macdougall, J.D., 1990. Geochemistry and isotopic characterization of mafic (Phulad Ophiolite) and related rocks in Delhi Supergroup, Rajasthan, India: implication of rifting in Proterozoic. Precamb. Res. 48, 167–191.

Walsh, J.N., Buckley, F., Barker, J., 1981. The simultaneous determination of the rare-earth elements in rocks using inductively coupled plasma source spectrometry. Chem. Geol. 33, 141–153.

Weil, A.B., Van der Voo, R., MacNiocall, C., Meert, J.G., 1998. The Proterozoic Supercontinent Rodinia: paleomagnetically derived reconstructions for 1100 to 800 Ma. Earth Planet. Sci. Lett. 154, 13–24.

Wiedenbeck, M., Goswami, J.N., 1994. High precision $^{207}Pb/^{206}Pb$ zircon geochronology using a small ion microprobe. Geochim. Cosmochim. Acta 58, 2135–2145.

Wiedenbeck, M., Goswami, J.N., Roy, A.B., 1996. Stabilization of the Aravalli Craton of northwestern India at 2.5 Ga: an ion microprobe study. Chem. Geol. 129, 325–340.